International Journal of Mechanical Engineering and Technology (IJMET)
Volume 10, Issue 02, February 2019, pp. 289-301, Article ID: IJMET_10_02_030
Available online at http://www.iaeme.com/ijmet/issues.asp?JType=IJMET&VType=10&IType=2
ISSN Print: 0976-6340 and ISSN Online: 0976-6359

LAPLACE TRANSFORM DECONVOLUTION AND ITS APPLICATION TO WELL TEST DATA ANALYSIS

Olabode O. A
Department of Petroleum Engineering, Covenant University, Nigeria

Sangotade I. M
Department of Petroleum Engineering, University of Ibadan, Nigeria

Afolabi A. O and Egeonu G. I.
Department of Petroleum Engineering, Covenant University, Nigeria,

ABSTRACT

The primary objective of this project is to extend the conveniences of deconvolution to non-linear problems of fluid flow in porous media. Unlike conventional approaches, which are based on an approximate linearization of the problem, here the solution of the non-linear problem is linearized by a perturbation approach, which permits term-by-term application of deconvolution. Because the proposed perturbation solution is more conveniently evaluated in the Laplace-transform domain and the standard deconvolution algorithms are in the time-domain, an efficient deconvolution procedure in the Laplace domain is a prerequisite.

For this research objective, a new algorithm is introduced which uses inverse mirroring at the points of discontinuity and adaptive cubic splines to approximate rate or pressure versus time data. This algorithm accurately transforms sampled data into Laplace space and eliminates the Numerical inversion instabilities at discontinuities or boundary points commonly encountered with the piece-wise linear approximations of the data.

Applying the algorithm to the field data obtained from published works, we can unveil the early-time behavior of a reservoir system masked by wellbore-storage effects. The wellbore-storage coefficient can be variable in the general case. The new method thus provides a powerful tool to improve pressure-transient-test interpretation.

Practical use of the algorithm presented in this research has applications in a variety of Pressure Transient Analysis (PTA) and Rate Transient Analysis (RTA) problems. A renewed interest in this procedure is inspired from the need to evaluate production performances of wells in unconventional reservoirs. With this approach,

we could significantly reduce the complicating effects of rate variations or shut-ins encountered in well-performance data

Keywords: Deconvolution, Well Testing, Sand Face, Pressure, Laplace transformation, well bore storage, cubic splines.

Cite this Article: Olabode O. A, Sangotade I. M, Afolabi A. O and Egeonu G. I., Laplace Transform Deconvolution and its Application to well Test Data Analysis, *International Journal of Mechanical Engineering and Technology*, 10(2), 2019, pp. 289-301.
http://www.iaeme.com/IJMET/issues.asp?JType=IJMET&VType=10&IType=2

1. INTRODUCTION

In conventional well-test analysis, the pressure response to constant-rate production is essential information that presents the distinct characteristics for a specific type of reservoir system however, in many cases, it is difficult to acquire sufficient constant-rate pressure-response data. The recorded early-time pressure data are often hidden by wellbore storage (variable sand-face rate) in some cases, outer boundary effects may appear before wellbore-storage effect disappears. Therefore, it is often imperative to restore the pressure response in the absences off wellbore storage effects to provide a confident well-test analysis

There are three main reasons for sand face rate variation: these are:

1. Well bore storage (referred to as after flow in buildup)
2. Lack of control of the surface rate
3. Cross flow between layers in multilayer testing.

The main focus of this project is to extend the conveniences of the deconvolution to non-linear problems of fluid flow in porous media.

The usual to approach to extend deconvolution procedures to non-linear problems in oil and gas reservoirs is to linearize the non-linear diffusion equation in terms of a pseudo-pressure and then to apply the deconvolution. It is well known that the pseudo-pressure approach does not completely remove the nonlinearity, but, for practical purposes, the remaining nonlinearity is assumed to be weak and ignored. In this dissertation, the solution of the non-linear problem is obtained by a perturbation approach, which presents the solution as a series of solutions of linear problems. This approach permits term-by-term application of deconvolution. One practical problem still remains: The proposed perturbation solution is more conveniently evaluated in the Laplace-transform domain. The standard deconvolution algorithms, however, are in the time-domain. Thus, the development of an efficient deconvolution procedure in the Laplace-transform domain is a prerequisite to accomplish the main objective of this project. The approach taken in this work leads to the deconvolution of variable-rate data in the Laplace domain. Specifically, an approximate function is required to take sampled (tabulated) production rate and pressure data into Laplace domain. Furthermore, the step-changes in the production rate during shut-in periods lead to inaccuracy in approximating functions and instability in numerical Laplace inversion algorithms. In this study, a cubic-spline method with piecewise linear interpolation and boundary mirroring is developed in Laplace domain to approximate and transform the production rate and bottom-hole pressure into the Laplace domain. This algorithm accurately transforms sampled (tabulated) data into Laplace domain and eliminates the numerical inversion instabilities at discontinuous points or boundaries commonly encountered in the piecewise linear approximations of the data. The developed approach does not require modifications of scattered and noisy data or extrapolations of the tabulated data beyond the end values Rate and pressure measurements of wells usually include some level of noise, and due to the nature

of the deconvolution process (more specifically, deconvolution in Laplace domain), the computed underlying constant-rate response will display oscillations, which requires some degree of smoothing. To smooth the deconvolved pressure response, an adaptive approach using a Gaussian and Epanechnikov kernel regression is proposed. The adaptive kernel regression proposed herein is shown to be more successful than the normal kernel regression.

2. METHODOLOGY

Convolution and deconvolution

Laplace transformation of a function f(t) , defined for all $t > 0$, is given by

$$L\{\text{f (t)}\} = \text{f(s)} = \int_0^t 1\, e^{-st} f(t) dt \tag{1}$$

Where f(s), is the Laplace transformation of f (t) and s denotes the Laplace transform parameter. Convolution of two functions yields the algebraic product of the functions in Laplace domain as follows:

$$L\{(f_1 * f_2)(t)\} = L\left\{\int_0^t f_1(T) * f_2(t - \text{T})\right\} \text{dT} \tag{2}$$

Let *g(s)* and f(s) be the Laplace transforms of *g(t)* and *f(t),* respectively. Let *y (t)* be the convolution of *g(t)* and *f(t).* This can be expressed mathematically as:

$$y(t) = \int_0^t g(t - T) * f(T) dT \tag{3}$$

Y(s) is defined as the Laplace transform of *y (t),* so:

$$\bar{y}(S) = \bar{g}(S) * \bar{f}(S) \tag{4}$$

Which is the convolution expression in Laplace space. .

The convolution theorem can be used to determine a system response to any excitation, provided that its response to a step function perturbation is known. In the same way it is possible to find the pressure response of a reservoir-fluid system *Δp(t)* to a variable sandface rate *q(t),* from the pressure response ~p.(t) to a reference constant sandface rate qr

$$\Delta p(t) = \int_0^t \frac{q(T)}{q_r} * \Delta \acute{p}_r\,(t - T) dT \tag{5}$$

or the cumulative production response *Q(t)* of a system to a sand face pressure history ~p(t), from the accumulated production response $\acute{Q}_r$ corresponding to a constant sandface drawdown Δp_r

$$Q(t) = \int_0^t \frac{\Delta p(T)}{\Delta p_r} * \acute{Q}_r\,(t - T) dT \tag{6}$$

It should be mentioned that in Equations 4 and 5, the initial conditions are null, i.e.:

$$\Delta p_r(0) = 0$$

and

$$\Delta Q_r(0) = 0$$

The expressions for Equations 4 and 5 in Laplace space are, respectively

$$\overline{\Delta p}(s) = s * \frac{\bar{q}(s)}{q_r} * \overline{\Delta p_r} \tag{7}$$

$$\bar{Q}(s) = s * \frac{\overline{\Delta p}(s)}{\Delta p_r} * \overline{Q_r}(S) \tag{8}$$

As can be seen, the deconvolution in Laplace space is reduced to a mere arithmetic operation. If deconvolution in real time is desired, the implementation of numerical methods to solve Equations (7) and (8) are necessary.

For deconvolution in Laplace space for constant pressure response:

$$:\overline{\Delta p_c}(s) = \frac{\overline{\Delta p(s)}}{sq(s)} \tag{9}$$

3. LAPLACE TRANSFORMATION OF SAMPLED FUNCTIONS USING CUBIC SPLINES

Interpolation by polynomials of degree *n* is widely used in practice. For various functions, the higher quality of the interpolation might be expected with the increasing degree of the polynomials. Unfortunately, this is not always true and the interpolation may yield oscillatory results by higher-degree of polynomials. Losing the quality of the interpolation by using higher-degree polynomials has been discussed by [1] and [8]. To avoid such oscillations, spline methods are widely applied. The mathematical idea of the spline is to replace a single high-degree polynomial over the entire interval by several low-degree polynomials [2]. This is expected to reduce the oscillation of the interpolation. In general, a spline function is a function that consists of piecewise polynomials joined together with certain smoothing conditions. A spline function also utilizes the degree piecewise polynomials to preserve order derivatives at the data points. A spline function is defined by knots and the order of the spline. In the theory of splines, the points $t0, t1 \ldots\ldots tn$, at which the character of the function changes, are called knots.

In this work, the most popular piecewise polynomial, called the natural cubic spline, is utilized. The cubic spline preserves the first and second derivative continuity at knots. If s(t) is given over the interval $a \leq t \leq b$ with knots defined by

$$a < t1 < t2 < \cdots \ldots < tn$$

then the cubic spline in each subinterval can be written in the following form:

$$S_i(t) = A_{0i}t + A_{2i}t^2 + A_{3i}t^3, i = 1,2 \ldots\ldots n \tag{10}$$

The simplified cubic splines function for each subinterval with values and at and respectively can be address in the form of (Atkinson, 1985)

$$S_i(t) = \frac{(t_i-t)^3M_{i-1}+(t-t_{i-1})^3M_i}{6(t_i-t_{i-1})} + \frac{(t_i-t)y_{i-1}+(t-t_{i-1})y_i}{(t_i-t_{i-1})} - \frac{1}{6}(t_i - t_{i-1})\{(t_i - t)M_{i-1} + (t - t_{i-1})M_i \tag{11}$$

In Eq.(11), M represents the second derivative and . Eq. (11) can also be rearranged as follows:

$$S_i(t) = \frac{M_i-M_{i-1}}{6(t_i-t_{i-1})}t^3 + \frac{3t_iM_{i-1}-3t_{i-1}M_i}{6(t_i-t_{i-1})}t^2 + \left[\frac{3(t_{i-1}^2M_i-3t_i^2M_{i-1}}{6(t_i-t_{i-1})} + \frac{y_i-y_{i-1}}{t_i-t_{i-1}} + \frac{1}{6}(t_iM_{i-1} - t_iM_i - t_{i-1}M_{i-1} + t_{i-1}M_i)\right]t + \left[\frac{t_i^3M_{i-1}-t_{i-1}^3M_i}{6(t_i-t_{i-1})} + \frac{t_iy_{i-1}-t_{i-1}y_i}{t_i-t_{i-1}} - \frac{1}{6}(t_i^2M_{i-1} - t_it_{i-1}M_i - t_{i-1}t_iM_{i-1} + t_{i-1}^2M_i\right] \tag{12}$$

4. GOVERNING EQUATIONS IN LAPLACE DOMAIN

Applying Eq. (1) on cubic spline over the interval $t1 < t < tn$ for tabulated data, such as pressure or production rate, yields

$$L\{S(t)\} = \bar{S}(s) = \int_{0^-}^{\infty} S(t)e^{-st}dt = \int_{0^-}^{t_1} S(t)e^{-st}dt + \int_{t_1}^{t_n} S(t)e^{-st}dt + \int_{t_n}^{\infty} S(t)e^{-st}dt = \int_{t_1}^{t_n} S(t)e^{-st}dt \quad (13)$$

For the set of tabulated data for both terms and vanish because the cubic spline becomes zero outside the interval. Application of Eq.(13) to individual terms of Eq.(12) yields:

The Laplace transform of the first term:

$$L\left\{\frac{M_i - M_{i-1}}{6(t_i - t_{i-1})}t^3\right\} = \int_{t_0}^{t_n} \frac{M_i - M_{i-1}}{6(t_i - t_{i-1})}t^3 e^{-st}dt =$$

$$\int_{t_0}^{t_1} \frac{M_1 - M_0}{6(t_1 - t_0)}t^3 e^{-st}dt + \int_{t_1}^{t_2} \frac{M_2 - M_1}{6(t_2 - t_1)}t^3 e^{-st}dt + \ldots. \int_{t_{n-1}}^{t_n} \frac{M_n - M_{n-1}}{6(t_n - t_{n-1})}t^3 e^{-st}dt =$$

$$\sum_{i=2}^{n} \frac{M_i - M_{i-1}}{6(t_i - t_{i-1})}\{[-\frac{t_i^3}{s} - \frac{3t_i^2}{s^2} - \frac{6t_i}{s^3} - \frac{6}{s^4}] - [-\frac{t_{i-1}^3}{s} - \frac{3t_{i-1}^2}{s^2} - \frac{6t_{i-1}}{s^3} - \frac{6}{s^4}]e^{-st_{i-1}}\} \quad (14)$$

The Laplace transform of the second term:

$$L\left\{\frac{3t_iM_{i-1} - 3t_{i-1}M_i}{6(t_i - t_{i-1})}t^2\right\} =$$

$$\int_{t_0}^{t_n} \frac{3t_iM_{i-1} - 3t_{i-1}M_i}{6(t_i - t_{i-1})}t^2 e^{-st}dt = \int_{t_0}^{t_1} \frac{3t_1M_0 - 3t_0M_1}{6(t_1 - t_0)}t^2 e^{-st}dt + \ldots.. \int_{t_{n-1}}^{t_n} \frac{3t_nM_{n-1} - 3t_{n-1}M_n}{6(t_n - t_{n-1})}t^2 e^{-st}dt =$$

$$\sum_{i=2}^{n} \frac{3t_iM_{i-1} - 3t_{i-1}M_i}{6(t_i - t_{i-1})}\left\{\left[-\frac{t_i^2}{s} - \frac{2t_i}{s^2} - \frac{2}{s^3}\right]e^{-st_i} - \left[-\frac{t_{i-1}^2}{s} - \frac{2t_{i-1}}{s^2} - \frac{2}{s^3}\right]e^{-st_{i-1}}\right\} \quad (15)$$

5. INVERSE MIRRORING AT BOUNDARIES

Discontinuous points in sampled data, such as step changes in production rate or build up in the pressure data, may cause oscillations in the approximation functions obtained (for example, by cubic spline). Transforming the data into the Laplace domain with such oscillations in the approximation function increases the error in the deconvolved constant pressure response. Figure 1 shows an example of the oscillatory behavior around discontinuous points caused by the application of cubic-spline approximation of the data. In addition, sampled functions are normally available over a finite interval while Laplace transformation requires the function be defined over the positive semi-infinite domain. To take the sampled data to Laplace domain, extrapolation from zero to the first sampling point and from the last sampling point to infinity is required. If the behavior of the tabulated function beyond the endpoints is known [e.g. constant wellbore storage, radial flow, pseudo steady state, etc. [3], then the Laplace transform of the function can be generated by the procedures suggested by [4] and [5]. As previously noted, however, due to the property of the cubic spline, the Laplace integration over the regions of extrapolation vanishes. To remove the remaining oscillations of the approximating function at discontinuity points, we propose the use of inverse mirroring at these points. In this approach, the function is extended beyond the points of discontinuity by using its inverse mirror image and the cubic-spline interpolation is applied to each extended function obtained by individual inverse mirroring. This reduces the oscillations of the function known as the tail effect. Figure 2 shows an example of inverse

mirroring at discontinuous points. Figure 3 shows the interpolation results from the application of the inverse mirroring and cubic spline. (50,100,200)

6. ADAPTIVE CUBIC SPLINE

Inverse mirroring at discontinuous points can be also used to extend the sampled data at both ends of the table where the behavior of the function is unknown. In this case, the two discontinuous points are the two ends of the data set. Figure 2 shows an example of inverse mirroring at the data boundaries of an arbitrary function. The inverse mirroring at the first data point may create negative values. These data points are rejected while transforming the extended function into the Laplace domain.

Field data may not be as smooth as was shown in Figure 3. The oscillatory nature of the field data may cause the same effect as discontinuities on the cubic spline interpolation. The application of inverse mirroring for the entire set of data in these cases would make the procedure impractical. Using inverse mirroring only at the two ends of the data set as shown in Figure 4 may be a partial solution for this problem. Inverse mirroring at the first data point is used to fill the gap from zero to first data point. However, It is used in the last data point to shift the tail effect may occur during Laplace inversion to the right.

An alternative solution for data with discontinuity at any point between the first and last data points is to use an ***adaptive cubic spline*** approach. In the adaptive cubic spline approach, piecewise linear approximations are substituted for the function in intervals where the cubic spline approximation causes large oscillations. The mathematical expression of the Laplace transformation of the piecewise linear approximations used in selected segments are as follows:

The equation of a straight line over a segment can be written as:

$$y = mx + b \tag{16}$$

Where m is the slope of the line passing through knots over a particular segment, and b represents the intercept of the line.

Slope for a particular line between two knot can be determined from the following relation

$$m = \frac{y_i - y_{i-1}}{t_i - t_{i-1}} \tag{17}$$

Similarly, the intercept of the line can also be found as follow

$$b = y_{i-1} - mt_{i-1} = y_{i-1} - \frac{y_i - y_{i-1}}{t_i - t_{i-1}} t_{i-1} \tag{18}$$

The Laplace transformation of a piecewise-linear function over an interval from to is then written as follow:

$$L\{y(t)\} = \bar{y}(s) = \int_{t_{i-1}}^{t_1} y(t)\, e^{-st} dt = \int_{t_{i-1}}^{t_1} (mt + b)\, e^{-st} dt = \int_{t_{i-1}}^{t_1} mt\, e^{-st} dt + \int_{t_{i-1}}^{t_1} b\, e^{-st} dt = m\left[\left(\frac{-t_i}{s} - \frac{1}{s^2}\right) e^{-st_i} - \left(\frac{-t_{i-1}}{s} - \frac{1}{s^2}\right) e^{-st_{i-1}}\right] - \frac{b}{s}\left[e^{-st_i} - e^{-st_{i-1}}\right] \tag{19}$$

Where m and b are given in Eq. (18) and Eq.(19), respectively.

7. ISEGER ALGORITHM

A newer algorithm presented by [6] removes the restriction on discontinuities. The Iseger algorithm is based on Poisson's summation formula in the form of Fourier series. In this algorithm, Poisson's summation relates an infinite sum of Laplace transform values to Z-transforms of the function's values. The infinite sum is approximated by a finite sum based on the Gaussian quadrature rule, and the time domain values of the function are computed by a

Fourier Transform algorithm [3]. The practical application of Iseger's algorithm in transient-flow problems was introduced by [3].

Den Iseger algorithms derive from the inverse Laplace transform definition:

$$f(t) = \frac{1}{2\pi i}\int_{\gamma-i\infty}^{\gamma-i\infty} \exp(pt)\, F(p)dp \qquad .(20)$$

Where γ is such that the contour of integration is to right-hand side of any singularities of F.

After algebraic manipulation, (6) may be expressed as follows:

$$\boldsymbol{f(t)} = \frac{\mathbf{1}}{\mathbf{2}\pi i}\boldsymbol{exp}(\gamma t)\int_0^{+\infty} Re\{F(p)\exp(iwt)\}dw \qquad (21)$$

Where *P is* From a trapezoidal rule with a step □/T, it follows that the time domain solution can be approximated by:

$$f(t) \approx \frac{1}{2\pi}\exp(\gamma t)[\frac{F(\gamma)}{2} + \sum_{k=1}^{+\infty} Re\left\{F\left(\gamma + \frac{ik\pi}{T}\right)\exp\left(\frac{ik\pi t}{T}\right)\right)\}]\pi \qquad (22)$$

7.1. SIMULATED EXAMPLES

7.1.1. Deconvolution of Pressure Responses for a Sequence of Step-Rate Changes

To demonstrate the use of the adaptive cubic spline in deconvolution applications, we consider the step-rate sequence and corresponding bottomhole pressure in Figure 5 and Figure 6, respectively. The pertinent data for this example are given in Table 1. For this variable-rate (step-rate changes) example, we used the Laplace domain deconvolution given in Eq. (9) to generate the constant rate responses (with wellbore storage) shown in Figure 7. The Laplace transformation of the tabulated pressure responses,$\Delta p_w(t)$, were generated by the adaptive cubic spline algorithm combined with an analytical solution for tabulated production rate. The Iseger numerical Laplace inversion algorithm is utilized in this example.

7.2. FIELD EXAMPLES

One field examples of the adaptive cubic-spline deconvolution will be presented herein. It is a the classical examples of [7] which deal with variable sandface flow rate due to wellbore storage effect.

7.3. Sandface Rate Deconvolution – [7] Example

The first standard example is an 8-hour buildup test with after flow effects considered by [7]. In this example, the underlying dual-porosity reservoir behavior is masked by wellbore storage and the objective of deconvolution is to reveal the underlying reservoir behavior. Figure 8 shows the original data and the deconvolved pressure response. Adaptive cubic spline, inverse mirroring, adaptive kernel regression, and Iseger numerical inversion algorithm are employed in this example. The results from adaptive cubic spline deconvolution and adaptive kernel regression display the valley in derivative responses, which is characteristic of dual-porosity systems (the depth of the valley is used to estimate the storativity ratio of the dual-porosity medium). The valley in the derivative responses was masked in the original data by wellbore storage. The results of both the fixed and the adaptive bandwidth utilized in kernel regression are shown in Figure 8. The fixed bandwidth value used in kernel regression was obtained from cross-validation to avoid over smoothing. A discussion on how over smoothing can affect the storativity estimation in this example is given by [3].

8. CONCLUSION

Laplace transformation is an important tool for the solution of transient fluidflow problems in porous media and the,existence of accurate numerical Laplace,inversion algorithms greatly

Enhances its utility. In the study, the main objective was to improve the deconvolution of variable-rate data in the Laplace domain. The main hypothesis of the first objective was that the limited success of Laplace-domain deconvolution and transformation of tabulated data into Laplace domain was due to algorithmic issues. Laplace transform was applied to the cubic spline equation to get the governing equation in laplace space. A governing equation can also be derived by implementing a design of experiment on all the functioning parameters. This will generate a response surface equation as described by [9] and can be applied to a cubic spline.

8.1. NOMENCLATURE

b	intercept on y axis used in equation
f_i	Value of at time f(t) at T_i
$f(t)$	Arbitrary function
$\overline{f(s)}$	Laplace transform of $f(t)$
f_s'	Linear slope of the data in the interval $t_i \leq t \leq t_{i+1}$
h	Constant kernel bandwidth parameter and reservoir thickness
$g(x\|h)$	Nadaraya-Watson kernel estimator
$h(x_i)$	Adaptive bandwidth
J	Arithmetic average of data
k	Kernel function
L	Characteristic length, ft
$\mathfrak{L}$	Laplace transform operator
$\mathfrak{L}^{-1}$	Inverse Laplace transform
M	Number of points at which the inverse Laplace transforms are computed
m	slope of a straight line used in eq. (3.15)
n	parameter used in the stehfest algorithm
P_i	Initial reservoir pressure, psi
P_{wD}	Dimensionless bottom hole pressure
Δp_{wc}	Constant rate pressure response, psi
$\overline{\Delta p}_{(s)}$	Pressure changes in Laplace space
$\bar{Q}_{(s)}$	Production rate in Laplace space, rbbl/d, stb/d
q	Production rate
S_i	Cubic spline over a segment
S	skin factor
T	Period for which the inversions are computed
t	Time, hrs

8.2. GREEKS

α	Constant used in Eq. (2.3)
α_0	Constant used in Eq. (2.3)
γ	Contour of integration
B	Constant used in Eq. (2.3)
β_0	Constant used in Eq. (2.3)
μ	Viscosity, cp
η	Diffusivity constant, md-psi/cp
λ_i	Bandwidth adaptive parameter
σ	Standard deviation and dispersion parameter
Δ	Parameter used in Iseger algorithm
Γ	Gamma function

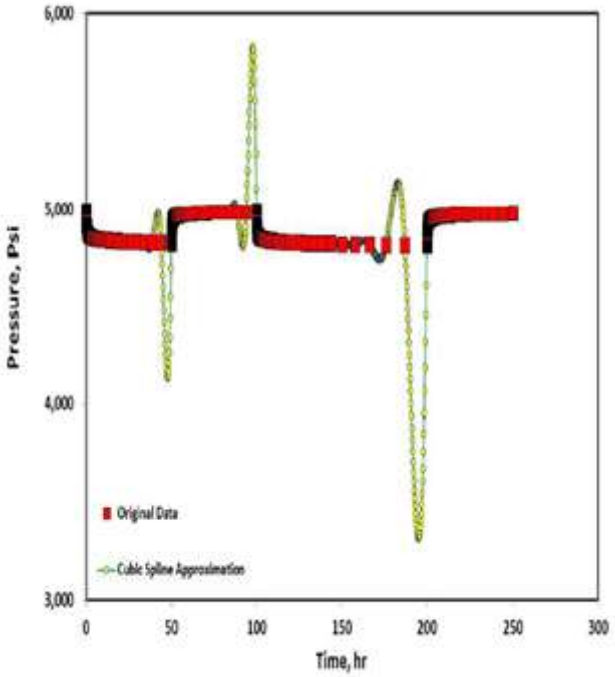

Figure 1 Interpolation of discontinuous pressure data

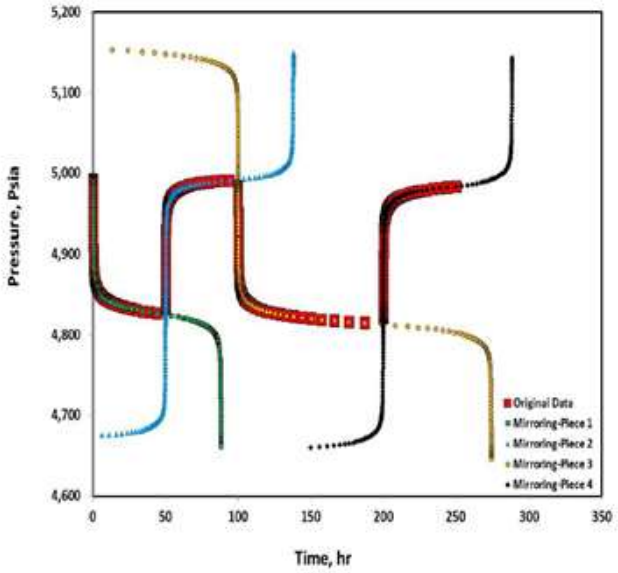

Figure 2 inverse mirroring at discontinuous point

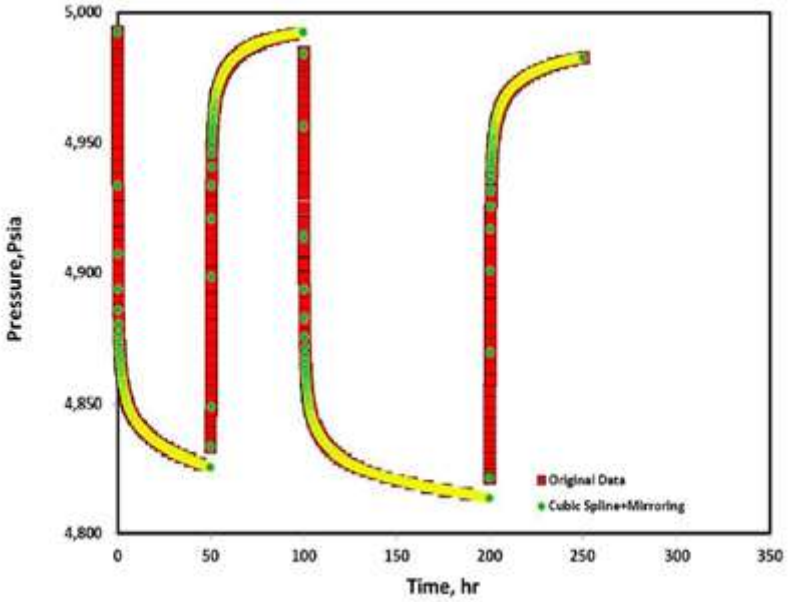

Figure 3 Application of inverse mirroring at discontinuous points using cubic spline interpolation.

Table 1 **Data for deconvolution example**

r_w ft	p_i psi	μ cp	ϕ fraction	c_t psi^{-1}	h ft	kh md.ft	S_f	C bbl/psi	B rbbl/stb
0.3	5000	1	0.1	3.00E-06	30	1000	0.0	0.01	1

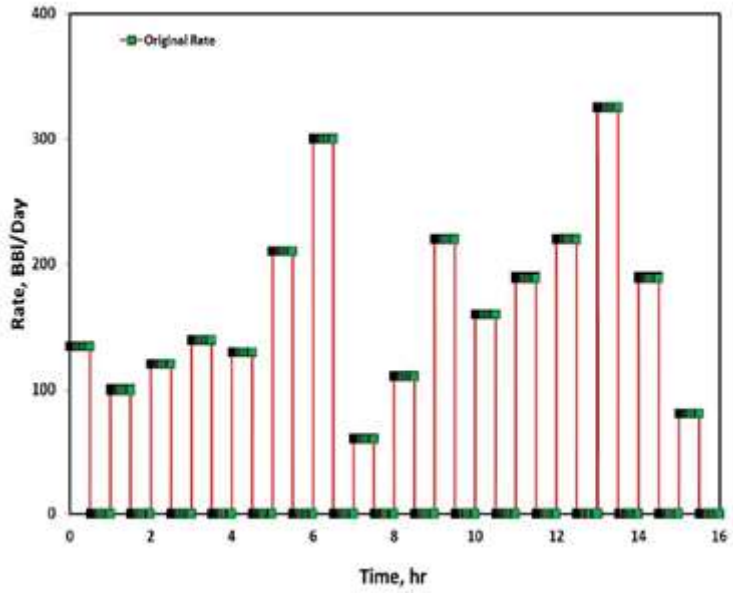

Figure 1 step-rate changes

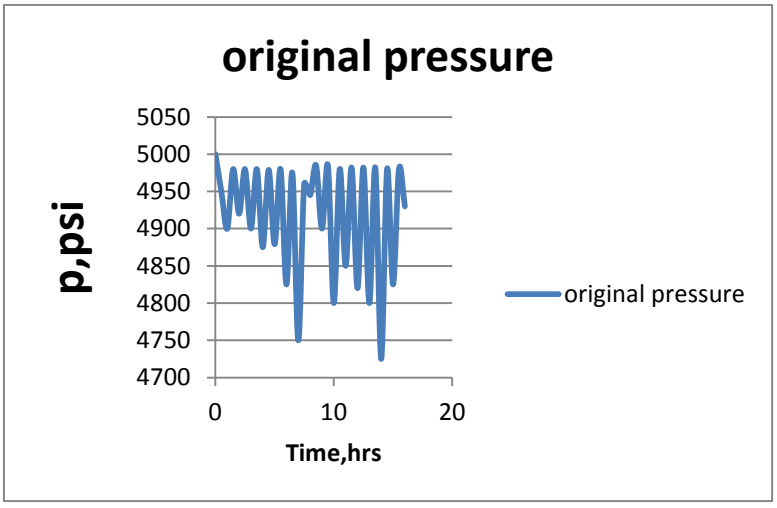

Figure 5 Pressure corresponding to step-rate sequence shown in Figure 4

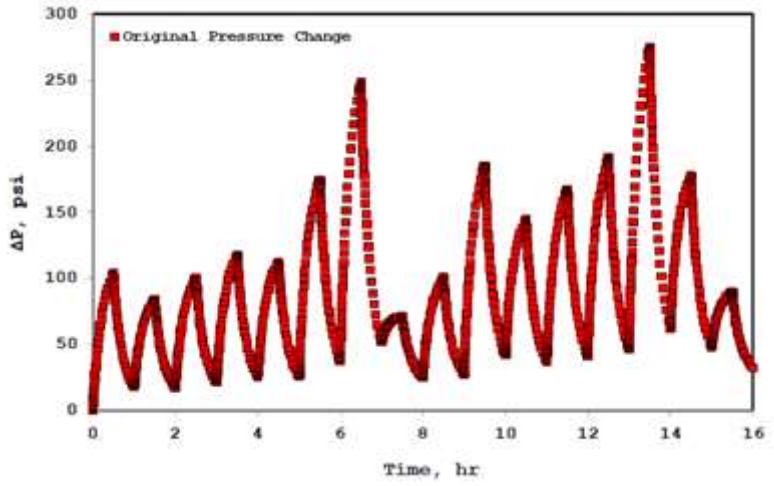

Figure 6 Pressure changes corresponding to step-rate sequence shown in Figure 4

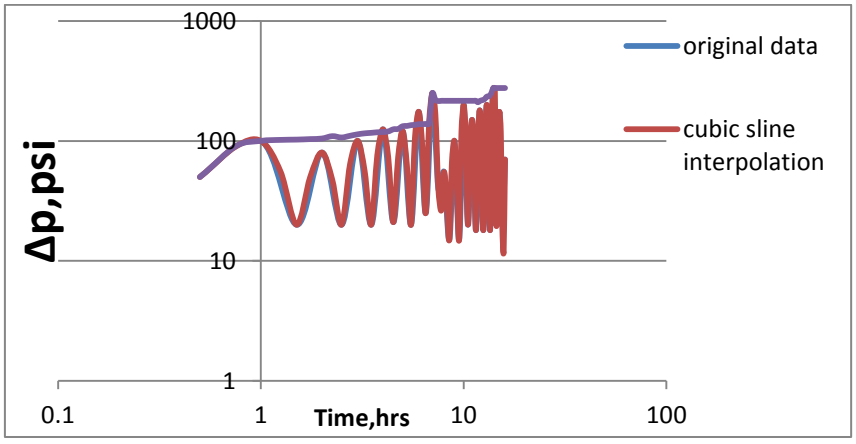

Figure 7 Deconvolution of pressure response

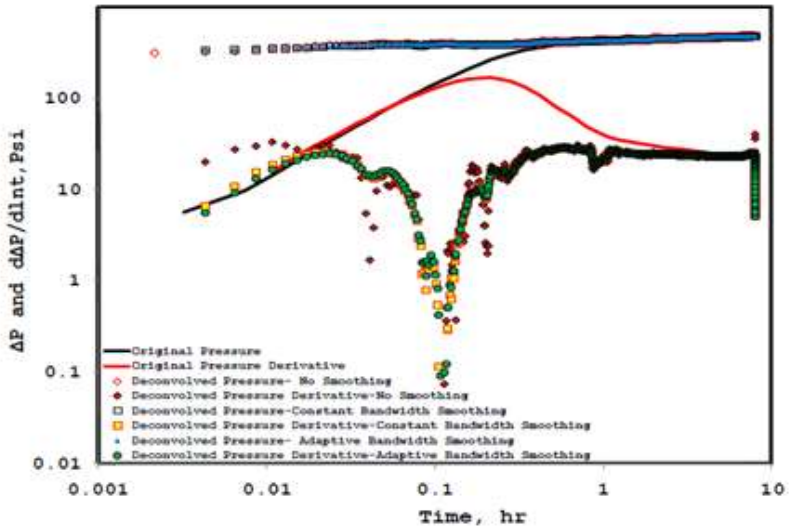

Figure 8 Sand face-rate deconvolution to remove wellbore storage effect; Muenuier et al. (1985) example

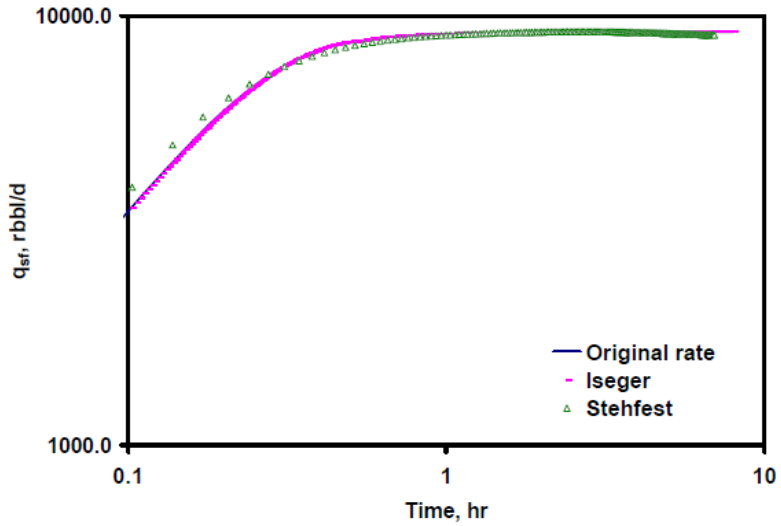

Figure 9 Numerical inversion of sand face rate from tabulated data. Muenuier et al. (1985) example.

ACKNOWLEDGEMENT

The authors wish to thank the Management of Covenant University for the support and funding.

REFERENCES

[1] Krayszig, E. 1999. Advanced Engineering Mathematics. John Wiley & Sons, INC.

[2] De Boore, C. 2001. A Practical Guide to Splines. Applied Mathematical Sciences, Vol 27.

[3] Al-Ajmi, N., Ahmadi, M., Ozkan, E., and Kazemi, H.2008. Numerical Inversion of Laplace Transforms in the Solution of Transient Flow Problems with Discontinuities. Paper SPE 116255 at SPE Annual Technical Conference and Exhibition. Denver, CO, 21-24 Sep.

[4] Roumboutsos, A. and Stewart, G. 1988. A Direct Deconvolution or Convolution Algorithm for Well-Test Analysis. Paper SPE 18157 presented at the SPE Annual Technical Conference and Exhibition. Houston, TX. 2-5 Oct.

[5] Onur, M. and Reynolds, A. C. 1998. Numerical Laplace Transformation of Sampled Data for Well-Test Analysis. SPE REE (June): 268-277.

[6] Iseger, P. D. 2006. Numerical Transform Inversion Using Gaussian Quadrature. Probability in the Engineering and Informational Sciences, 20. 1-44.

[7] Meunier, D., Wittmann, M. J., and Stewart, G. 1985. Interpretation of Pressure Buildup Test Using In-Situ Measurement of Afterflow. JPT (Jan.): 143-152.

[8] Optimal side track time evaluation by proxy model, G. I. Egeonu, O. D. Orodu, **O. A. Olabode**, Pet Coal (2017); 59(6):747-761 ISSN 1337-7027 . Open access journal.*

[9] Effect of foam and WAG (water alternating gas) injection on performance of thin oil rim reservoirs, **Olabode O. A**, Orodu O. D., Isehunwa S., Mamudu A., Rotimi T., Journal of Petroleum Science and Engineering, 2018.*